Hall Thruster Discharge Chamber Plasma Characterization Using a High-Speed Axial Reciprocating Electrostatic Probe

James M. Haas[§], Richard R. Hofer[§] and Alec D. Gallimore[¶]
Plasmadynamics and Electric Propulsion Laboratory
Department of Aerospace Engineering
The University of Michigan
College of Engineering
Ann Arbor, MI 48109

ABSTRACT

Electron temperature, number density, plasma potential and floating potential were measured in the interior and very-near-field region of the P5 Hall thruster using the newly developed High-speed Axial Reciprocating Probe (HARP) positioning system. The HARP system was used to insert an electrostatic triple probe axially into the discharge chamber from 152 mm downstream of the exit plane to within 5 mm of the anode face, maintaining residence times under 100 ms. Probe data, discharge current and cathode potential were recorded continuously during probe movement; the latter two quantities verified the HARP system's limited perturbation to thruster operation. A second, slower, linear table was used to vary the radial location of the probe between axial sweeps resulting in a 2-D mapping of the chamber. Two thruster operating conditions were considered: 300 V, 5.3 A and 100 V, 5.3 A. At 300 V, a very complex plasma structure was observed. Regions of high electron temperature and plasma potential were observed near the anode and along the outer wall of the channel. Number density peaked on centerline near the region of high temperature and again downstream of the exit plane. A large accelerating potential was shown to exist outside the discharge chamber, agreeing with LIF ion velocity measurements at the exit plane. At 100 V, the coherent structure is largely absent which is expected based on the thruster's poor performance at this condition.

NOMENCLATURE

r_p	electrode radius
r_{Le}	electron Larmor radius
r_{Li}	ion Larmor radius
dx	electrode spacing
λ_D	Debye length
r_p / λ_D	Debye ratio
λ_{ii}	ion-ion collision mean free path
λ_{ee}	electron-electron mean free path
λ_{ei}	electron-ion mean free path
A_i	electrode area
V_i	electrode potential
e	fundamental electron charge
k_b	Boltzmann's constant
Te	electron temperature
n_e	electron number density
m_e	electron mass
M_i	ion mass
V_b	bias voltage
V_p	plasma potential
V_{sh}	current shunt voltage

INTRODUCTION

Over the past several years, U.S. interest in Hall thrusters for military, commercial and scientific uses has increased dramatically. Initial efforts to develop flight qualified thrusters centered on the 1.5 kW class thrusters for stationkeeping applications. More recently, the range of power levels has expanded as new missions are developed which can significantly

[§] Graduate Student, Aerospace Engineering, Student Member AIAA
[¶] Associate Professor, Aerospace Engineering and Applied Physics, Associate Fellow AIAA

benefit from the unique performance characteristics of Hall thrusters. Of particular interest to both industry and the government are Hall thrusters of the 5 kW range for orbit transfer missions. This interest and the need for a dedicated laboratory model thruster for diagnostics drove the development of the University of Michigan - Air Force Research Lab P5, 5 kW Hall thruster.

The University of Michigan's Plasmadynamics and Electric Propulsion Laboratory (PEPL) has developed a wide range of diagnostics providing a wealth of information on the plasma characteristics of Hall thruster plumes.[1-4] However, these diagnostics are limited to the region downstream of the thruster discharge chamber. They therefore do not provide any direct information on plasma parameters or ionization and acceleration mechanisms inside the thruster. This information is necessary if a better understanding of Hall thruster physics is to be obtained. This will allow for performance improvements and serve as a reference for validating numerical models.

An electrostatic triple probe was chosen to map the plasma parameters in the discharge chamber of the P5. Electrostatic probes are one of the simplest and most commonly used plasma diagnostic tools and are unique in the information they are capable of providing. They have found widespread use in the electric propulsion field[5-9] as well as nuclear fusion[10] and atmospheric and space sciences.[11] Electrostatic probes have been used successfully to measure electron temperature, number density, floating potential, and plasma potential in the plume of Hall thrusters downstream of the exit plane where particle densities and temperatures are relatively low.[12] However, upstream of the exit plane, the power density increases significantly, creating difficulties in taking measurements. Probe lifetime becomes severely limited in the discharge chamber environment and the probe's effect on the parameters it is attempting to measure becomes an issue. On time scales much less than that of probe lifetimes, the flux of high-energy particles in electric propulsion devices will sputter and/or heat the probe material causing it to ablate. Local plasma characteristics are then affected through emission of relatively cold probe material. These local variations propagate through the plasma, perturbing thruster operation.

The HARP system is designed specifically to address these concerns. The role of the HARP system is to enable electrostatic probe measurements within the Hall thruster discharge chamber with minimum perturbation to the surrounding plasma. Any probe of finite dimension must perturb the plasma to some extent to make measurements. However, keeping the residence time of the probe inside the chamber short can minimize the effects due to material ablation/sputtering. Probe heating due to the high-energy particle flux inside a Hall thruster has been estimated in previous work[13] for a cylindrical probe composed of tungsten with an alumina insulator. Including enhanced heating due to the Hall current, an ablation time on the order of 100 ms was predicted. Experimental results showing ablation times under 0.5 s tend to support these predictions. Using the thermal model ablation time prediction as a guideline, a high speed reciprocating probe positioning system was assembled with the ability to insert and remove electrostatic probes from the Hall thruster discharge chamber on time scales under 100 ms. This is still orders of magnitude greater than the response time of the probe which is on the order of the ion plasma frequency.[9] Such short residence times will assure probe survivability and limit perturbations to the local plasma and thruster operational parameters. This paper presents the initial findings of an experimental effort to map the plasma properties in the discharge chamber.

EXPERIMENTAL SET-UP

The purpose of this experiment was to characterize the plasma parameters in the very-near-field region and inside the discharge chamber of a Hall thruster, while avoiding significant perturbation to the thruster. Two operating conditions were considered. The first was at 100 V and 5.3 A, right on the I-V characteristic "knee",[12] corresponding to a condition of poor performance. The second was at 300 V and 5.3 A, in the ionization saturation region of the current-voltage characteristic. Comparison of the plasma structure at these two conditions yielded information on the acceleration and ionization mechanism of the thruster.

Vacuum Chamber

All experiments were conducted in the University of Michigan's 6 m diameter by 9 m long Large Vacuum Test Facility (LVTF). The pumping system consists of four CVI model TM-1200 Re-Entrant Cryopumps providing a measured xenon pumping speed of 140,000 l/s and an ultimate base pressure of 2×10^{-7} Torr. The operating pressure was 5.5×10^{-6} Torr when corrected for Xenon. The facilities have been described in detail in a previous work.[12]

Thruster

The thruster used was the University of Michigan – Air Force Research Lab P5 5 kW laboratory model Hall thruster. This thruster was developed specifically for improved diagnostic access. Compared to a 1.35 kW thruster, the larger discharge chamber of the P5 provides better spatial access for electrostatic probes as well as a lower power density that reduces the heat flux to the probe. The thruster has been thoroughly characterized and its performance closely matches that of commercially available 5 kW thrusters. Thrust, specific impulse, efficiency, and plasma parameter profiles in the plume are presented in a previous work.[12] To date, the P5 has accrued over two hundred hours of stable run time and continues to operate exceptionally well. The hollow cathode used, provided by the Moscow Aviation Institute (MAI), employs a small disk of lanthanum hexaboride as a thermionic emitter.

Positioning System

The HARP system is a linear motor assembly providing direct linear motion at very high speed and acceleration. It consists of a linear, "U"-shaped magnet track and a "T"-shaped coil moving on a set of linear tracks. There is no leadscrew to limit acceleration and speed as in traditional tables. The only contact between moving parts is through the guide rails, providing very little resistance. A linear encoder built into the magnet track provides position feedback for motion control. The table was covered by a stainless steel shroud to protect it from direct impact of ions while measurements were made. This prevented the motor from being excessively heated, which would have lead to performance degradation.

Triple Probe

A schematic of the triple probe chosen for this experiment is shown in Figure 1.

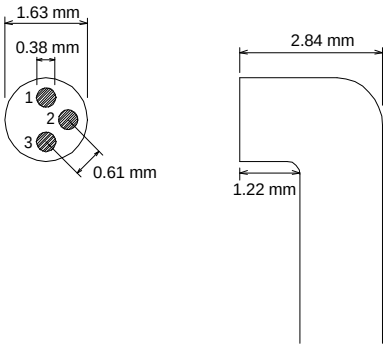

Figure 1. Triple probe schematic.

The probe consisted of three planar, tungsten electrodes insulated from each other and the plasma by a length of alumina tubing. Each electrode was 0.38 mm in diameter and the probe was configured such that the normal of the electrode surface was directed radially inward when positioned inside the thruster. Planar probes were chosen because of the limited area comprising the discharge chamber. Their small size offered much greater spatial resolution and ease of construction when compared to cylindrical probes. Electrode size was chosen based on the expected electron temperature and number density such that standard planar probe theory applied.[21] These assumptions are summarized below.

1. Unmagnetized ions

$$r_{Li} >> r_p \tag{1}$$

2. Thin sheath

$$\lambda_D < r_p \tag{2}$$

3. Collisionless plasma

$$\lambda_{ii} \approx \lambda_{ee} \approx \lambda_{ei} >> r_p \tag{3}$$

4. Probe spacing avoids electrode interaction

$$dx > \lambda_D \tag{4}$$

5. Unmagnetized electrons

$$r_{Le} < r_p \tag{5}$$

Inside the discharge chamber, magnetic fields are large enough that electrons are magnetized and assumption 5 is violated in the strictest sense. The orbital motion of the electrons inside the sheath must then be taken into account when determining the current collected by the probe. In this experiment, however, the effect of magnetized electrons on current collection was determined to be negligible since the probe was constructed such that the normal to the surface of each electrode was oriented parallel to the magnetic field lines. Parallel to the field lines, electron motion is not constrained by the magnetic fields and is a function only of their random thermal energy and any electric fields present. A probe orientation parallel to the magnetic field lines minimizes the effect of the electron orbital motion. This orientation also eliminates problems

arising from the presence of a flowing stream of ions. There is no directed flux toward the electrode surface nor does a wake region exist which might reduce the effective collection area.[6] This allows the Bohm approximation for ion current collection to be used.

The equation for the total current to each planar electrode is the same as for the case of a cylindrical probe. Thus the triple probe theory of Chen and Sekiguchi[14], is used to determine electron temperature, number density and plasma potential by Equations 6-8:

$$\frac{1}{2} = \frac{1 - \frac{A_3}{A_1}\exp\left(-\frac{e|V_2 - V_1|}{k_b T_e}\right)}{1 - \exp\left(-\frac{e|V_3 - V_1|}{k_b T_e}\right)} \qquad (6)$$

$$n_e = \frac{\exp\left(1/2\right)\frac{I_3}{A_3}}{e\left(\frac{k_b T_e}{M_i}\right)^{1/2}\left(1 - \exp\left(-\frac{e|V_3 - V_2|}{k_b T_e}\right)\right)} \qquad (7)$$

$$V_p = V_2 + \left|\left(\frac{k_b T_e}{e}\right)\ln\left[\left(\frac{2\pi m_e}{M_i}\right)^{1/2}\exp\left(-1/2\right)\right]\right| \qquad (8)$$

In Equations 6-8, V_2 floats and V_1 and V_3 are biased above and below V_2, respectively. A schematic of the circuit is shown in Figure 2.

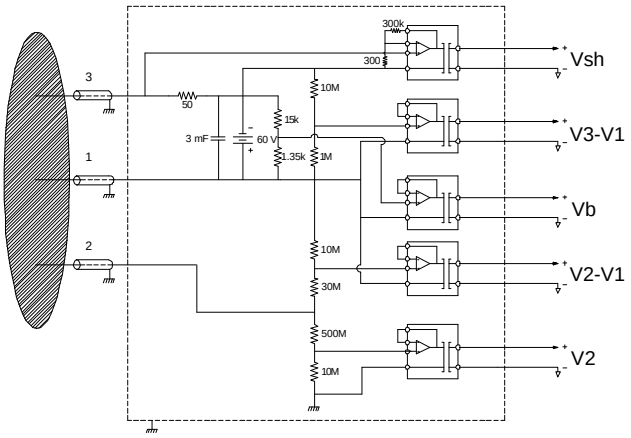

Figure 2. Triple probe circuit.

Large potentials inside the discharge chamber created significant difficulties in making measurements. The entire probe circuit floated to potentials of several hundred volts. A circuit was constructed based around the AD210 isolation amplifier. These amplifiers were capable of handling several thousand volts of common mode voltage and provided input impedances of 1×10^{14} Ω. The output of the isolation amplifiers connected to a LabView data acquisition system for data recording and storage.

Figure 3 shows the orientation of the probe and indicates the plane inside the thruster where plasma parameters were measured. The anode face is 5.1 mm upstream of the beginning of the mapped area and the exit plane is 33 mm downstream. The mapped area starts 1.3 mm from the inner wall and ends 3.8 mm from the outer wall. The cathode plane is located 50 mm downstream of the exit plane.

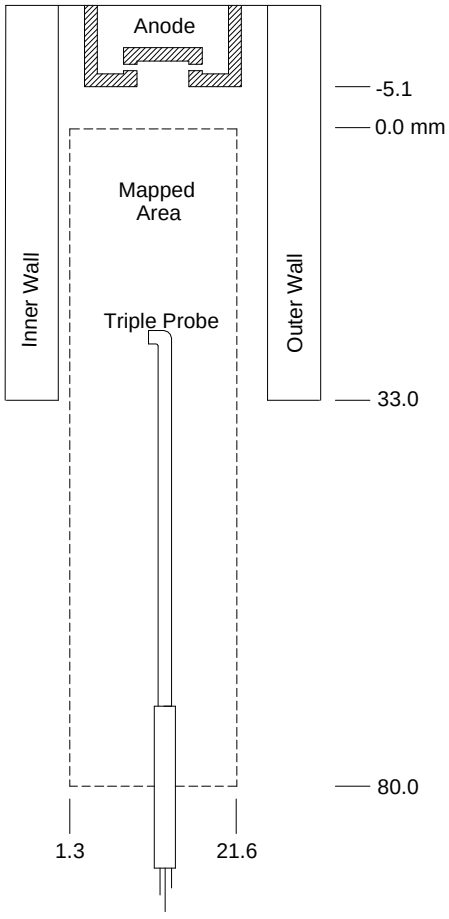

Figure 3. Mapped area inside and outside discharge chamber.

In order to minimize probe heating as much as possible, the probe home position was set 152 mm downstream of the exit plane. This location is the starting point for all axial sweeps. Data were recorded over the entire 185 mm sweep but only the first 80 mm of the data are presented to this study.

For the 100 V case, the criteria outlined above were met throughout the mapped region. At 300 V, however, extremely large temperatures and low densities resulted in criteria 2 and 4 approaching their limits throughout nearly the entire discharge chamber. Therefore, using theory outlined here, the accuracy of the 300 V data is diminished compared with the 100 V case. In this case, the data still provide a great deal of qualitative information about the plasma structure.

EXPERIMENTAL RESULTS

The initial phase of this experiment was the characterization of the HARP system's performance. Figure 4 shows a representative plot of position, velocity and acceleration versus time. From the plot, it can be determined that the total residence time inside the chamber is approximately 80 ms. This time varied slightly from stroke to stroke but always remained under 100 ms.

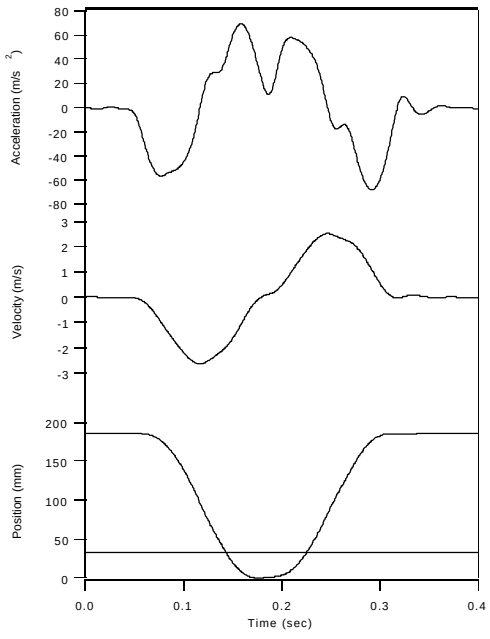

Figure 4. HARP system performance. Horizontal line on position plot indicates exit plane location.

The next phase of the investigation involved testing the extent of the probe's perturbation on thruster operation. Measurements were taken at the 300 V condition assuming probe ablation would be more pronounced than in the 100 V case. Previous tests[13] on an SPT-70 very clearly showed the significant perturbation an ablating probe has on various thruster parameters. Figure 5 illustrates the extent of this perturbation. The LVDT signal is a direct measure of the thrust while the PMT measures the photoemission from the ablating tungsten and alumina probe. Discharge current and cathode potential are also included.

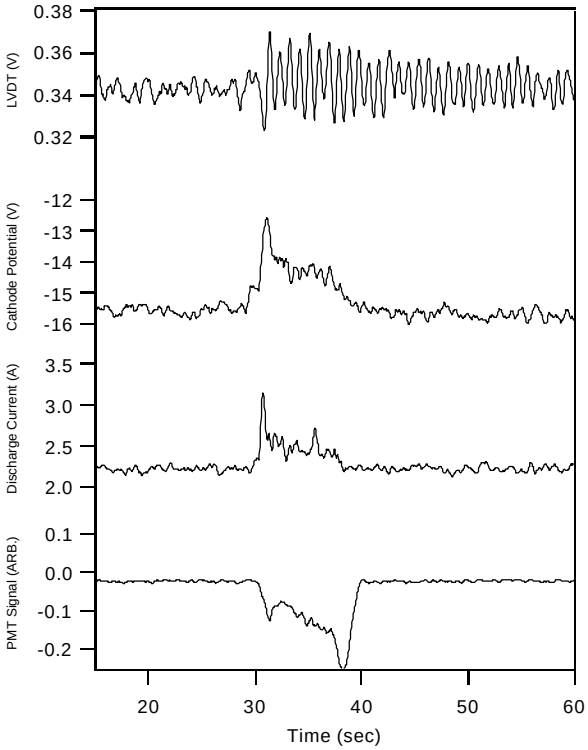

Figure 5. SPT-70 thruster parameter perturbation from a previous study.[13]

The data acquisition system used for the current investigation was limited to eight input channels, five of which were dedicated to the triple probe. Position feedback from the HARP system required one channel, leaving two free channels for thruster parameters. From the plots in Figure 5, probe ablation appeared to have the largest effect on discharge current and cathode floating potential. Therefore the remaining two data channels were used to monitor these parameters during all measurements.

Figure 6 is a sample raw data trace showing that discharge current and cathode potential remained completely unperturbed during the probe's sweep into and out of the discharge chamber. The data have not been corrected for the presence of voltage dividers in the circuit. The sample is taken at 300 V and 5.3 A and the same results were seen at 100 V and 5.3 A. The location of the exit plane is indicated by the vertical lines showing the portion of the trace corresponding to the probe being inside the thruster. Discharge current and cathode potential profiles were monitored for each data set and showed no perturbation during the entire experiment. Further, inspection of the probe after the tests revealed no obvious signs of material ablation.

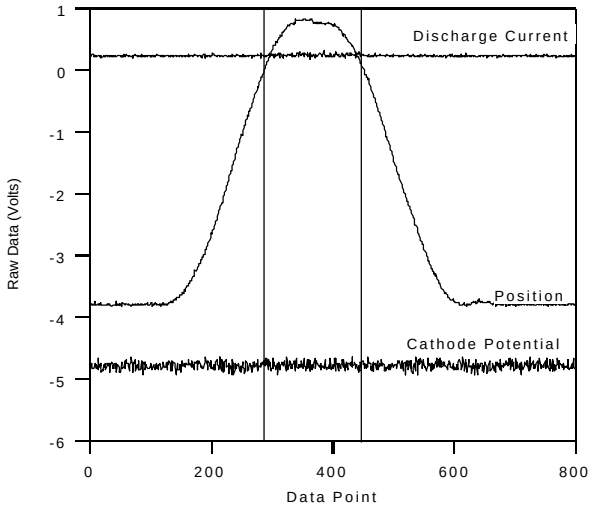

Figure 6. Discharge current and cathode potential profiles during probe sweep. The vertical lines indicate the exit plane location.

Figure 7 shows axial profiles of the plasma parameters at a radial position R = 14.0 mm from the inner chamber wall for the 300 V, 5.3 A case. Discharge chamber centerline is located at R = 12.7 mm. The zero axial position is 5.1 mm downstream of the anode and the exit plane is located at axial position A = 33 mm. The profiles are representative of data collected across the width of the discharge chamber.

Figures 8-12 are contour plots showing the Debye ratio (r_p/λ_d), electron temperature, number density, floating potential, and plasma potential at a thruster operating condition of 300 V and 5.3 A. The Debye ratio contours indicate the extent to which the thin sheath assumption is met in the discharge chamber. The plots cover the entire region inside the discharge chamber and extend 47 mm downstream of the exit plane. Note the "finger"-shaped region of high potential and temperature at the anode, near the inner wall.

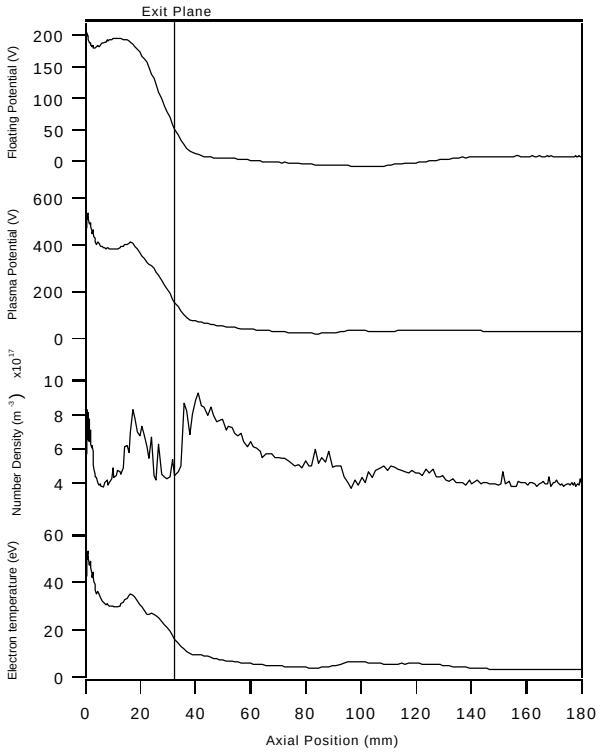

Figure 7. Representative axial profiles of plasma parameters at 300 V, 5.3 A at R = 14.0 mm. Discharge chamber centerline located at = 12.7 mm.

Figures 13-17 show the Debye ratio, electron temperature, number density, floating potential, and plasma potential for an operating condition of 100 V, 5.3 A. This condition occurs at the knee of the current-voltage characteristic and corresponds to low thruster efficiency. It also provided a less hostile environment in which to verify the operation of the triple probe and gives a point of comparison for the 300 V, 5.3 A case.

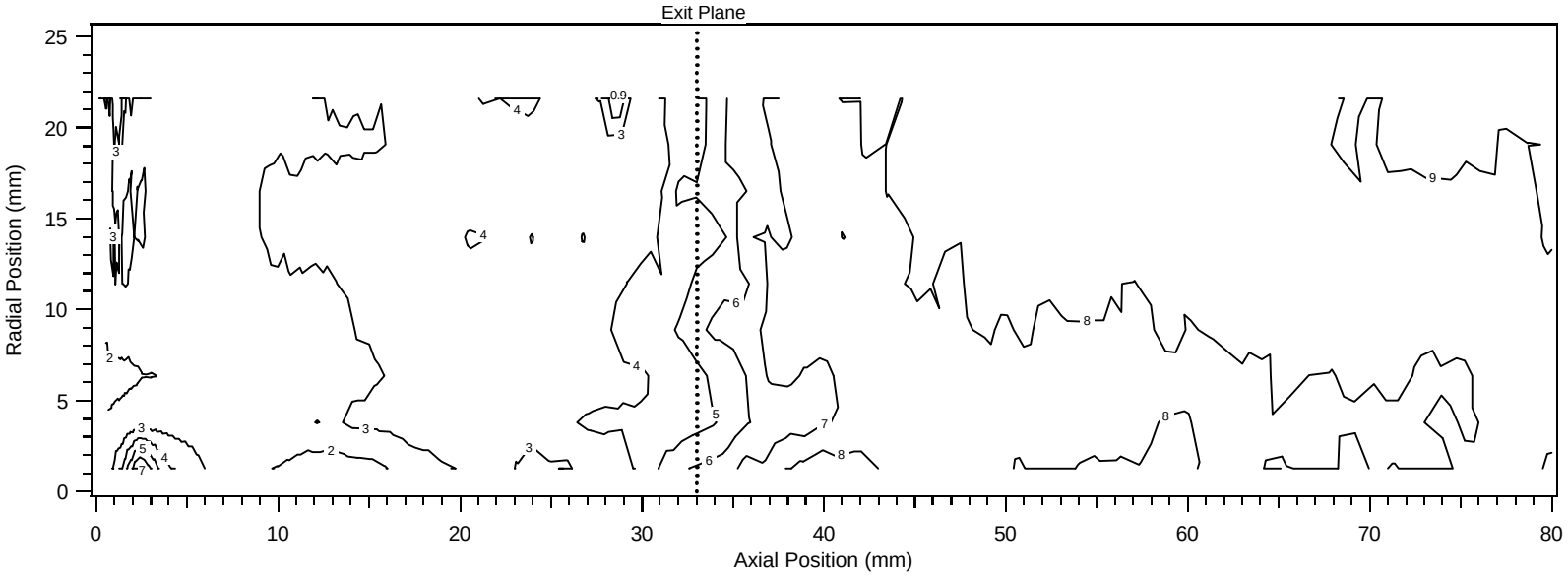

Figure 8. Debye ratio contours at 300 V, 5.3 A. Min. = 0.9 at (1.0,1.3).

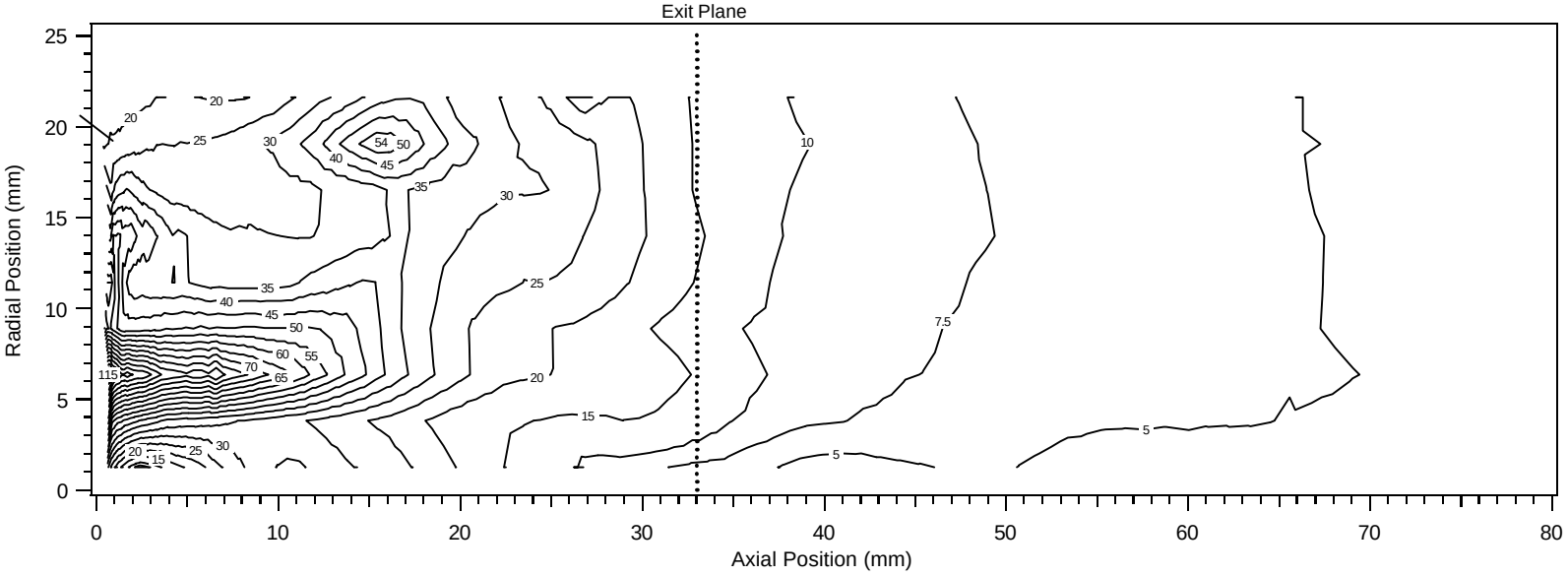

Figure 9. Electron Temperature (eV) contours at 300 V, 5.3 A. Max. = 115 eV at (0.8, 6.4).

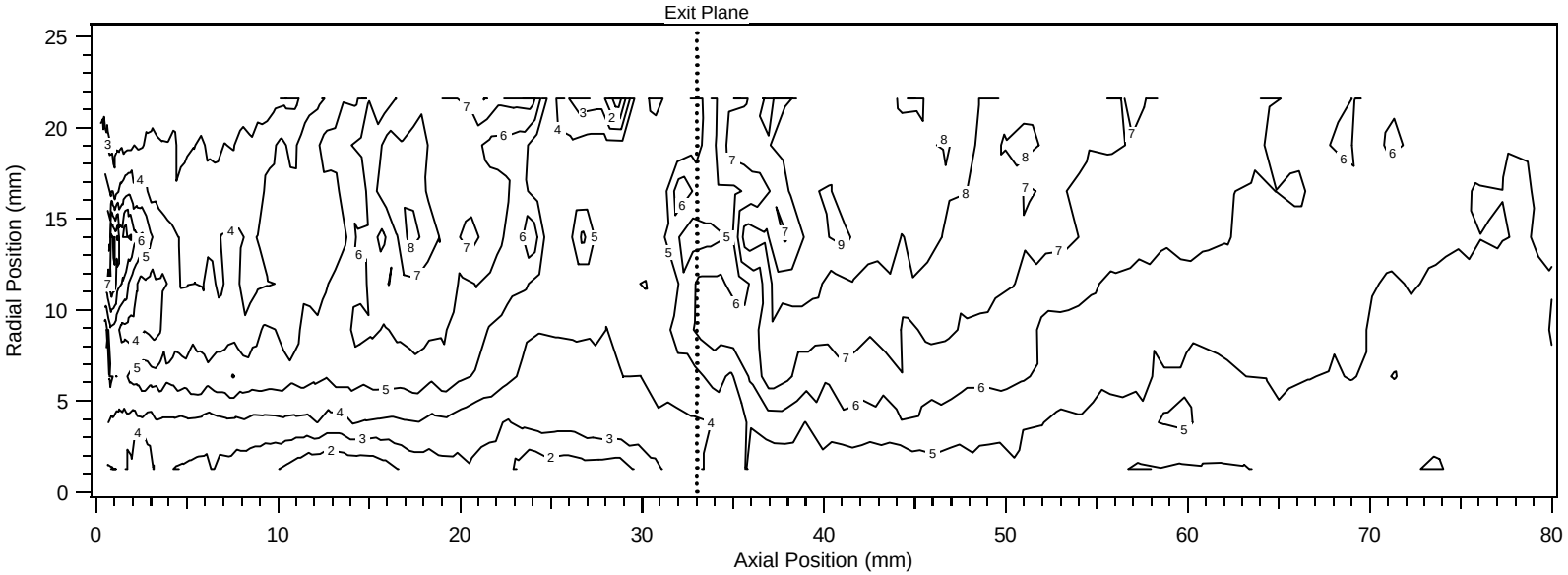

Figure 10. Number density (10^{17} m^{-3}) contours at 300 V, 5.3 A. Max. = 9x10^{17} m^{-3}.

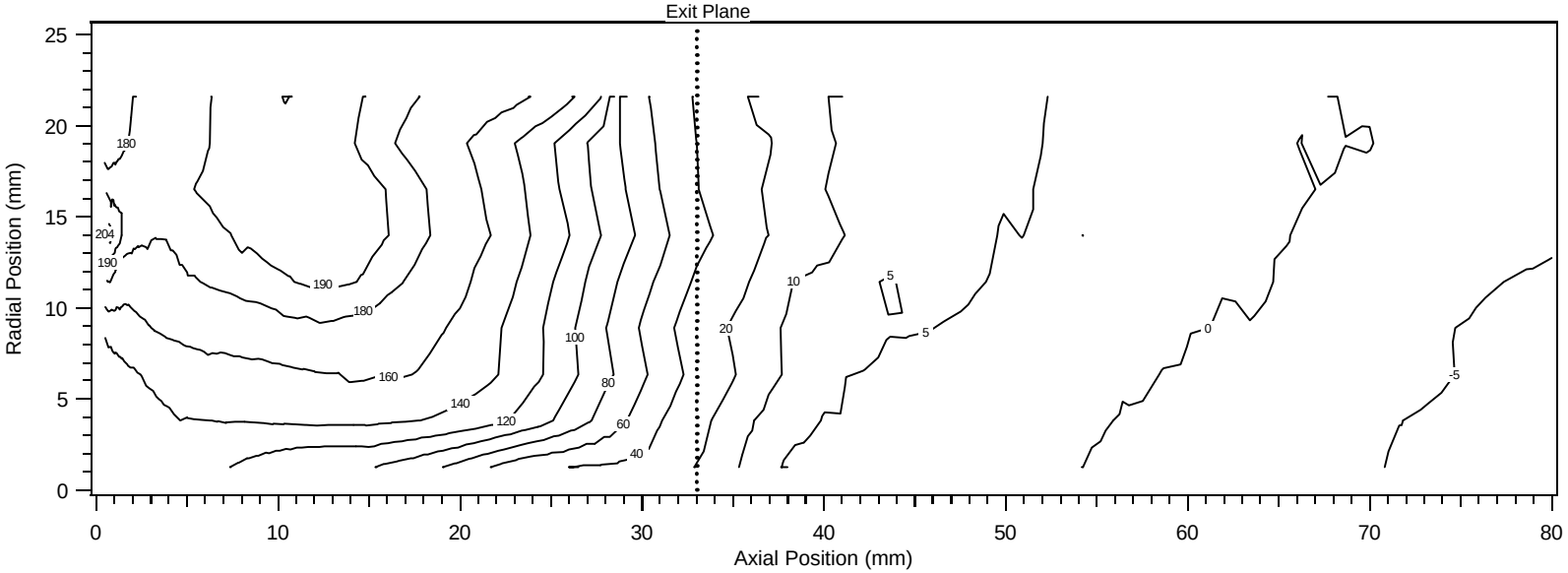

Figure 11. Floating potential (V) contours at 300 V, 5.3 A. Max. = 204 V at (1.8, 14.0).

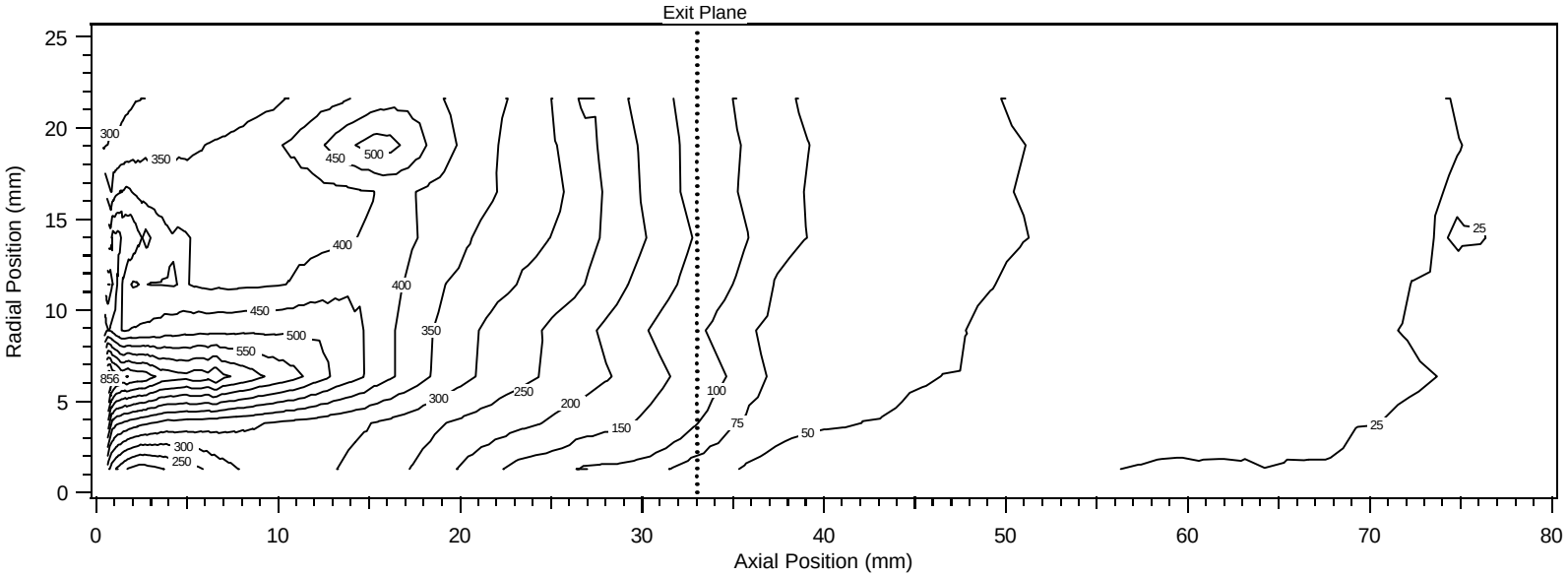

Figure 12. Plasma potential (V) contours at 300 V, 5.3 A. Max. = 856 V at (0.8, 6.4).

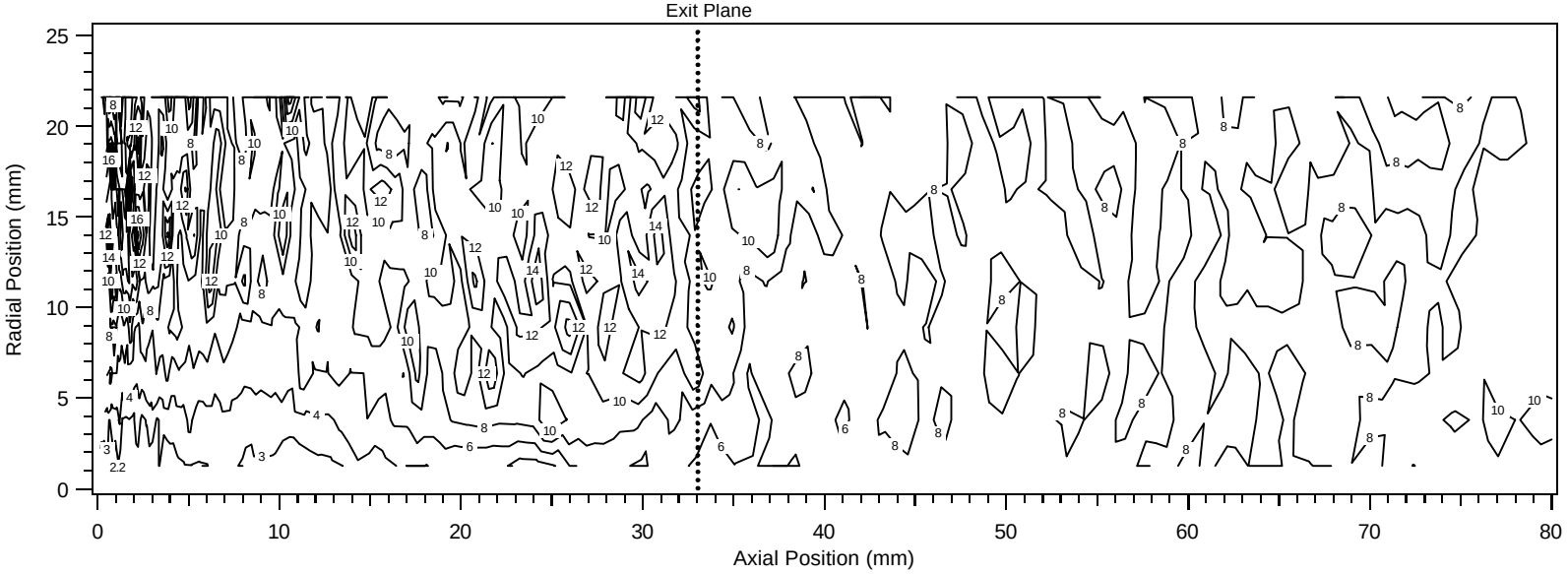

Figure 13. Debye ratio at 100 V, 5.3 A. Min. = 2.2 at (1.0,1.3).

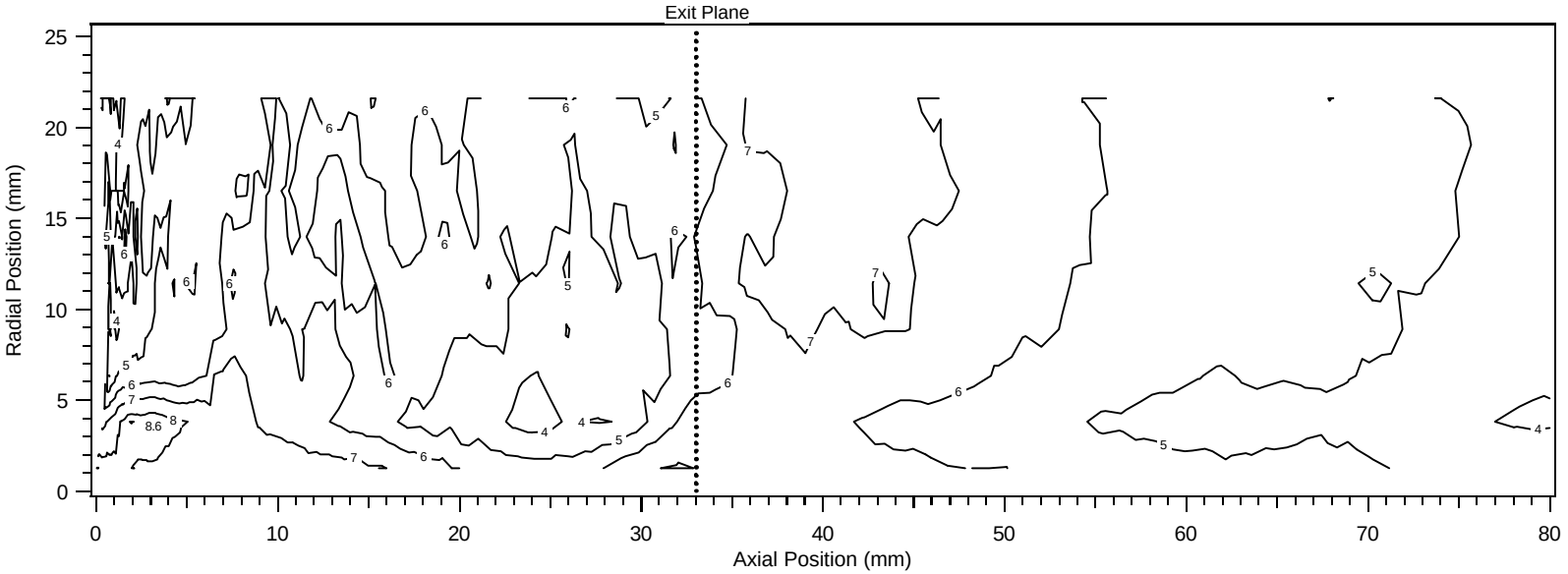

Figure 14. Electron temperature (eV) contours at 100 V, 5.3 A. Max. = 8.6 eV at (3.3, 3.8).

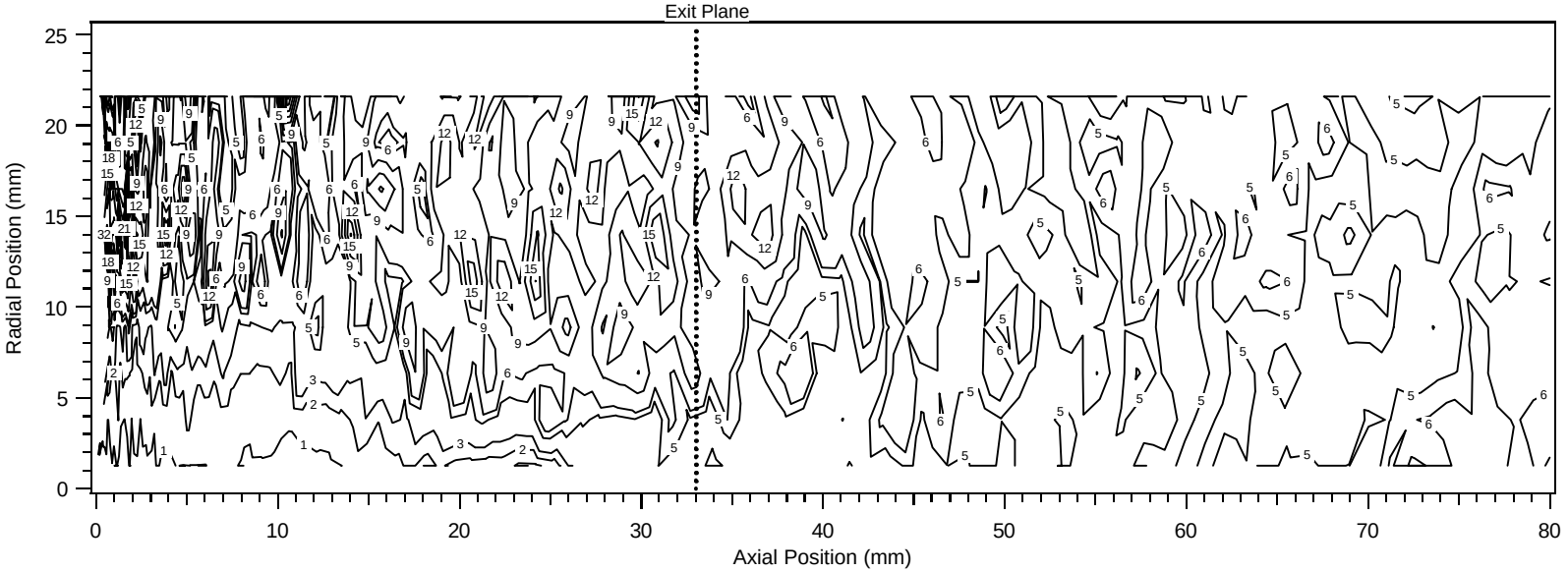

Figure 15. Number density (10^{17} m^{-3}) contours at 100 V, 5.3 A. Max. = 32x10^{17} m^{-3} at (0.7, 14.0).

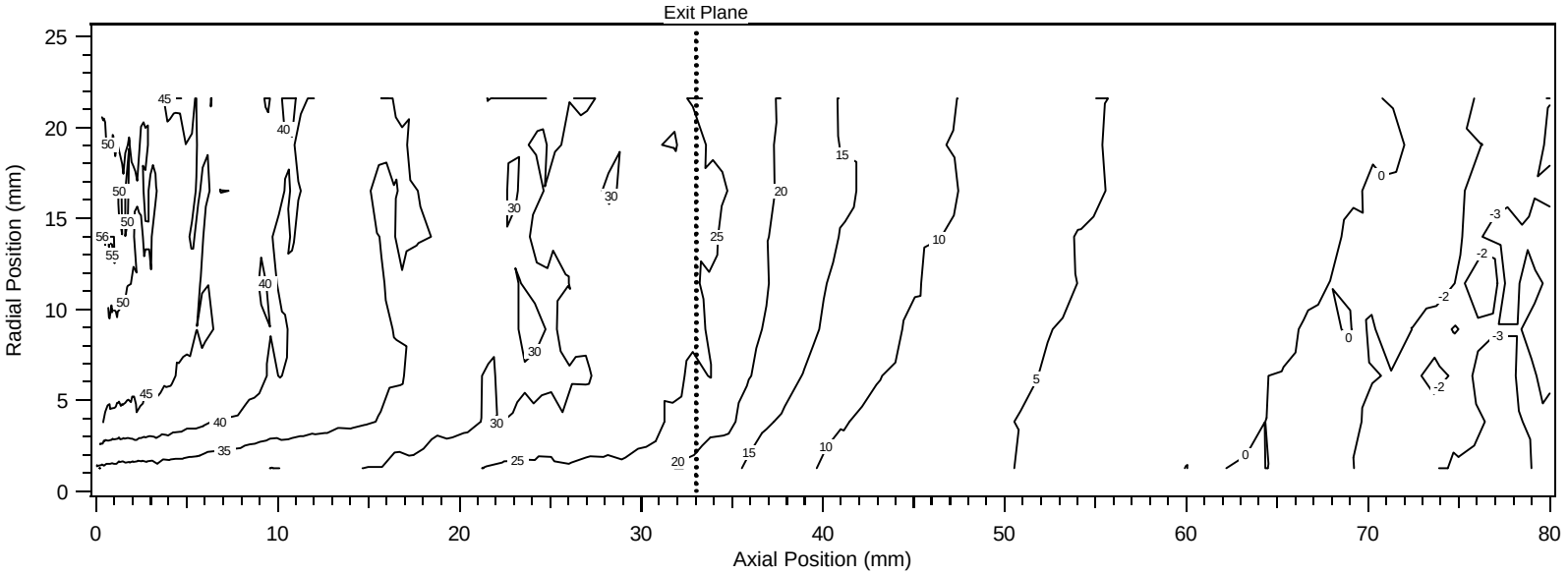

Figure 16. Floating potential (V) contours at 100 V, 5.3 A. Max. = 56 at (0.5, 14.0).

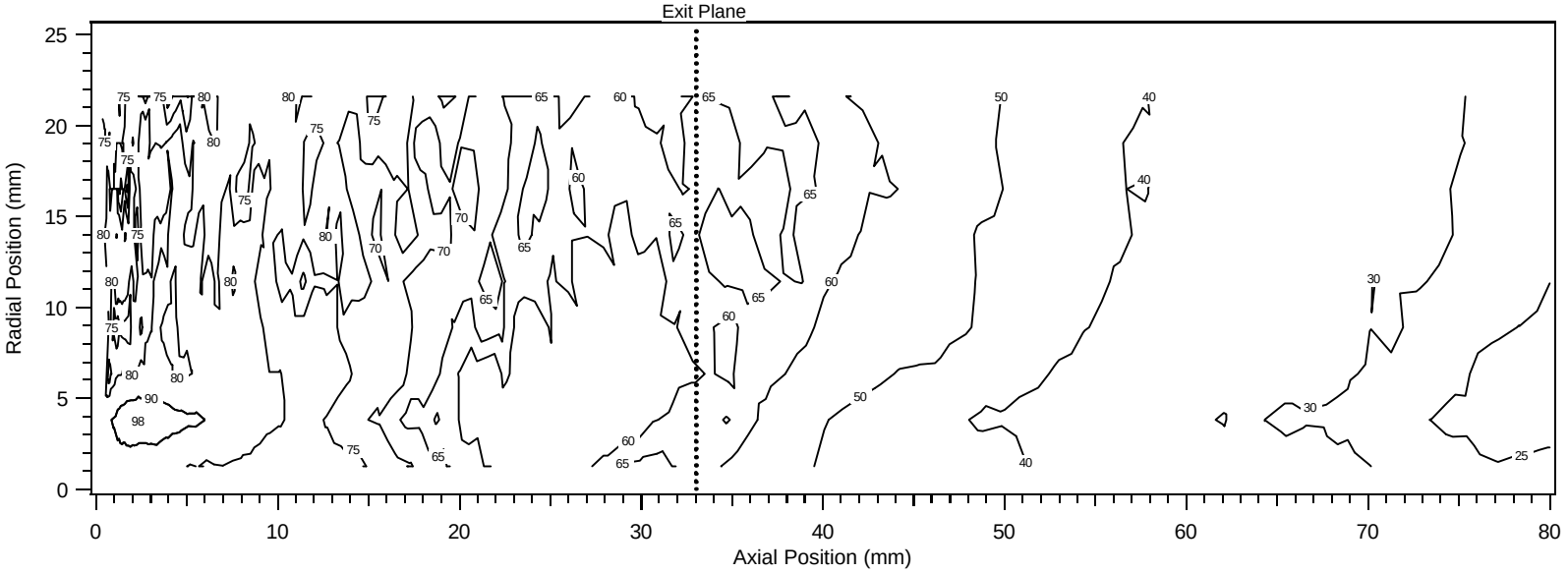

Figure 17. Plasma potential (V) contours at 100 V, 5.3 A. Max. = 98 V at (2.2, 3.8).

DISCUSSION

The results of this investigation have demonstrated the feasibility of making measurements inside the discharge chamber of a Hall thruster using a high-speed reciprocating probe. The HARP system confirms that if probe residence times inside the discharge chamber are minimized, the plasma may be interrogated without ablating significant probe material and perturbing thruster operation. Perturbation effects have been documented in the case of near-field measurements of a D-55 TAL[1] and an SPT-70.[13] However, measurements of this type made by a number of other researchers make no mention of thruster perturbation.[8,15,17] Figure 5 illustrates results from a previous investigation[13] showing the extent of perturbations that can occur. This investigation[13] provided ablation time estimates, giving a starting point for the design of a high-speed probe system to avoid these effects. Figure 4 shows the performance of this system and its ability to insert and remove the triple probe on time scales at or below 100 ms. Figure 6 shows a representative trace verifying that there are no significant thruster perturbations occurring during data collection.

Figure 9 shows the electron temperature contours for the 300 V case. The peak temperature observed is 115 eV and occurs 0.8 mm from the anode, 6.4 mm from the inner wall. Previous studies have reported maximum electron temperatures in the 20-30 eV range[8,22,23,24], a factor of 4-5 less than the maximum temperature observed in this study. However, this is not unexpected. Recall that for large residence times, significant material ablation has been observed. This ablated material cools the surrounding plasma resulting in artificially low electron temperature values. By keeping the residence time below 100 ms, this effect is mitigated and measured electron temperatures are correspondingly higher. The presence of higher energy electrons has been predicted theoretically.[23] Significant populations of higher energy electrons have also been measured experimentally[8] in the tail of the electron energy distribution function. Note that the highest temperatures occur away from the discharge chamber walls where secondary electrons and heat transfer cool the plasma. Temperatures also tend to be highest near the anode, which, unlike the ceramic chamber walls, does not moderate the temperature through low-energy secondary electron emission. These high temperatures lead to extremely large plasma potentials, as seen in Figure 12.

Figure 10 shows the number density contours in the mapped area. Of particular interest is the presence of two regions of high density along the centerline at 17 mm and 40 mm. Local maximums in density correspond to large ionization rates and can be expected to occur where electron temperatures are large. The local density maximum at 17 mm corresponds closely to a region of high electron temperature (54 eV), decreasing as the newly formed ions are accelerated downstream. Using similar logic, a large density of ions would be expected in the region of high temperatures near the anode but this does not agree with the measured values. This may be due to the lack of electron confinement in this region of weak magnetic fields. The second density peak occurs approximately 15 mm downstream. This agrees with data from near-field measurements of the SPT-100[19] where the density peak was attributed to the presence of the cathode. In general, the number density peaks radially near centerline, decreasing toward both the inner and outer walls. Axially, number density has a main peak 8-10 mm downstream of the exit plane implying this is a region of ionization. Measurements by Bishaev[24] show similar trends, however, they indicate the peak density occurs slightly upstream of the exit plane and no secondary peak inside the channel exists. Guerrini[8] provide centerline data that show a large increase in number density downstream of the exit plane, agreeing with results in Figure 10.

In Figure 12, the plasma potential exhibits a complex structure, the most striking aspect being the “finger”-shaped region extending out from the anode, off centerline, near the inner wall. The peak potential of 856 V, which is nearly three times the discharge voltage, is reached in this area. Such a large value is believed to be an artifact of the triple probe theory used here. However, the possibility of potential values exceeding the discharge voltage has not been ruled out due to the presence of ion backflow to the anode observed in other work.[15,24] Ion backflow is also implied in the current results where, in regions closer to the outer wall, the potential drop is towards the anode. Morozov[15] showed a potential structure which was very similar to the current results but differed in that it was much more uniform across the width of the discharge chamber. Near centerline, the plasma potential remains constant to within ~10% in the axial direction then begins to decrease approximately 20 mm downstream of the anode. This type of potential drop has been reported previously for centerline data[8] and for the width of the discharge chamber.[15,24] Finally, the finger structure implies

that ions will be accelerated to both the inner and outer walls of the channel.

Another interesting aspect of the plasma potential data is the indication that the ions experience approximately 100 V of accelerating potential outside the thruster. Laser Induced Fluorescence (LIF) measurements[16] 100 mm downstream of the exit plane indicate ions from this thruster, operating at 300 V, see a most probable accelerating potential of approximately 200 V. The same LIF measurements show an ion velocity at the exit plane equivalent to 100 V. The difference, 200 - 100 = 100 V, is in very good agreement with the 100 V of accelerating potential seen in these experiments. This type of acceleration region, extending well beyond the exit plane, is not unique[17], although Hall thrusters with ceramic discharge chambers (as opposed to a TAL) are generally considered to have an acceleration zone upstream of the exit plane.[15,18,24]

Figure 12 also shows the focusing effect on the ions outside the channel, which agrees with a number of observed thruster phenomena. Focusing ions along the axis of the thruster forms the dense beam in the center of the plume. Probe measurements show the presence of a low-density core on centerline near the exit plane[1,18,19] , which shrinks and eventually disappears further downstream. Ion energy analyzer measurements by Gulczinski[20] on the same thruster indicate the presence of high-energy ions directed at high angles (~90º) off thruster centerline. Gulczinski attributes this to ions being accelerated inward at high angles downstream of the exit plane, crossing the thruster axis and appearing as highly divergent ions on the opposite side.

Data collected at the 100 V and 5.3 A condition provided a relatively benign plasma in which to verify operation of the triple probe and the applicability of the specified probe theory. The 100 V case also provided a point of comparison for the 300 V operating condition. The 100 V case was chosen because it is at the current-voltage "knee", a region characterized by poor performance. This can be seen in the plasma contour plots in Figures 14-17 which show very little coherent structure. Electron temperature and number density are both fairly uniform throughout the channel with no pronounced decreases in density, which would be associated with an acceleration region. The presence of larger densities than in the 300 V case is a direct consequence of ions not being accelerated out of the channel. The plasma potential shows the same lack of coherent structure and hence no pronounced region of ion acceleration. These results are consistent with the poor performance observed at 100 V.

FUTURE WORK

Large temperatures (115 eV) and low densities ($6x10^{16}$) resulted in the thin sheath criteria approaching their limits throughout nearly the entire discharge chamber at 300 V. Future work will address this issue through a combination of new probe designs and development of probe theory more applicable to the region inside the discharge chamber. This will include better estimates of the effective current collection areas of the individual electrodes as well as improved models of the ion current density. Floating emissive probes will also be used to verify the triple probe results.

Future work will also include an extension of the mapping area. As is evident, significant acceleration occurs outside the channel, both axially and radially. To fully analyze and understand the ionization and acceleration mechanisms, the near-field region outside of the channel must be included. Also, probe orientation will be varied to measure the Hall current.

Finally, both high voltage and high current operating modes will be mapped out, providing information on the evolution of the plasma as operating conditions vary.

ACKNOWLEDGMENTS

The authors would like to thank their fellow students at the Plasmadynamics and Electric Propulsion Laboratory, Dr. Mitat Birkan of the Air Force Office of Scientific Research for his continued research support, and Sergei Khartov of MAI for the use of the LaB_6 cathode.

REFERENCES

1. Domonkos, M.T., et. al., "Very Near-Field Plume Investigation of the D55," AIAA 97-3062, July 1997.

2. Ohler, S., "Non-Intrusive Plasma Diagnostics for Electric Propulsion Research," AIAA 94-3297, June 1994.

3. Marrese, C.M., "D-100 Performance and Plume Characterization on Krypton," AIAA 96-2969, July 1996.

4. King, L.B., "Transport-property and Mass Spectral Measurements in the Plasma Exhaust Plume of a Hall-effect Space Propulsion System", Ph.D. Dissertation, University of Michigan, 1998.

5. Gallimore, A.D., et. al., "Near and Far-field Plume Studies of a 1 kW Arcjet," AIAA 94-3137, June 1994.

6. De Boer, P.T.C., "Electric Probe Measurements in the Plume of an Ion Thruster," Journal of Propulsion and Power, Vol. 12, No. 1, Jan.-Feb. 1996.

7. Burton, Rodney L., et. al., "Application of a Quadruple Probe Technique to MPD Thruster Plume Measurements," Journal of Propulsion and Power, Vol. 9, No. 5, Sept.-Oct. 1993.

8. Guerrini, G., et. al., "Characterization of Plasma Inside the SPT-50 Channel by Electrostatic Probes," IEPC 97-053, September 1997.

9. Tilley, Dennis L., et. al., "The Application of the Triple Probe Method to MPD Thruster Plumes," AIAA 90-2667, July 1990.

10. Rhodes, T.L., et. al., "Fast Reciprocating Probe System Used to Study Edge Turbulence on TEXT", Rev. Sci. Instrum., Vol. 61, No. 10, October 1990, pp. 3001-3003.

11. Seifert, W., et. al., "Methods for the Numerical Calculation of the Plasma Potential from Measured Langmuir Probe Characteristics", Contrib. Plasma Phys., Vol. 26, No. 4, 1986, pp. 237-254.

12. Haas, J.M., et. al., "Performance Characteristics of a 5 kW Laboratory Hall Thruster," AIAA 98-3503, July 1998.

13. Haas, J.M., et. al., "An Investigation of Electrostatic Probe Perturbations on the Operational Characteristics of a Hall Thruster and on the Measurement of Local Plasma Parameters," AIAA 98-3656, July 1998.

14. Chen, S-L, and Sekiguchi, T., "Instantaneous Direct-Display System of Plasma Parameters by Means of a Triple Probe," Journal of Applied Physics, Vol. 36, No. 8, August 1965, pp. 2363-2375.

15. Morozov, A.I., "Plasma Accelerator with Closed Electron Drift and Extended Acceleration Zone," Technical Physics, Vol. 17, No. 1, July 1972, pp. 38-45.

16. Williams, G.J., et al., "Laser Induced Fluorescence Measurement of Ion Velocities in the Plume of a Hall Effect Thruster," AIAA 99-2424, 35th Joint Propulsion Conference, June 1999.

17. Hargus, W.A., et. al., "A Study of a Low Power Hall Thruster Transient Behavior," IEPC 97-058, September 1997.

18. Kaufman, H.R., "Technology of Closed-Drift Thrusters," AIAA Journal, Vol. 23, No. 1, January 1985, pp. 78-87.

19. Kim, Sang-Wook, et. al., "Very-Near-Field Plume Study of a 1.35 kW SPT-100," AIAA 96-2972, July 1996.

20. Gulczinski, F.S., et. al. "Near-field Ion Energy and Species Measurements of a 5 kW Laboratory Hall Thruster," AIAA 99-2430, July 1999.

21. Schott, L., "Electrical Probes," from *Plasma Diagnostics*, Lochte-Holtgreven, W. (ed.), AIP Press, New York, 1995.

22. Askhabov, S. N., et. al., "Electric Discharge in Direct-Flow Hall Accelerator," Technical Physics, Vol. 22, No. 4, April 1977, pp. 453-458.

23. Baranov, V. I., et. al., "Energy Balance and Role of Walls in ACDE," IEPC 97-060, September 1997.

24. Bishaev, A. M., et. al., "Local Plasma Properties in a Hall-Current Accelerator with an Extended Acceleration Zone," Technical Physics, Vol. 23, No. 9, September 1977.